Evolutionary rescue model informs strategies for driving cancer cell populations to extinction

Amjad Dabi[1,*], Joel S. Brown[2,3], Robert A. Gatenby[2,3,4], Corbin D. Jones[5,6,7,*], and Daniel R. Schrider[1,7,*]

1. Department of Genetics, University of North Carolina, Chapel Hill, North Carolina, USA

2. Department of Cancer Biology and Evolution, Moffitt Cancer Center, Tampa, FL, USA

3. Department of Integrated Mathematical Oncology, Moffitt Cancer Center, Tampa, FL, USA

4. Diagnostic Imaging Department, Moffitt Cancer Center, Tampa, FL, USA

5. Department of Biology, University of North Carolina, Chapel Hill, North Carolina, USA

6. Integrative Program for Biological and Genome Sciences, University of North Carolina, Chapel Hill, North Carolina, USA

7. UNC Lineberger Comprehensive Cancer Center, University of North Carolina, Chapel Hill, North Carolina, USA

*corresponding authors: amjad_dabi@unc.edu, cdjones@email.unc.edu, drs@unc.edu

ABSTRACT

Cancers exhibit a remarkable ability to develop resistance to a range of treatments, often resulting in relapse following first-line therapies and significantly worse outcomes for subsequent treatments. While our understanding of the mechanisms and dynamics of the emergence of resistance during cancer therapy continues to advance, questions remain about how to minimize the probability that resistance will evolve, thereby improving long-term patient outcomes. Here, we present an evolutionary simulation model of a clonal population of cells that can acquire resistance mutations to one or more treatments. We leverage this model to examine the efficacy of a two-strike "extinction therapy" protocol, in which two treatments are applied sequentially to first contract the population to a vulnerable state and then push it to extinction, and compare it to a combination therapy protocol. We investigate how factors such as the timing of the switch between the two strikes, the rate of emergence of resistant mutations, the doses of the applied drugs, the presence of cross-resistance, and whether resistance is a binary or a quantitative trait affect the outcome. Our results show that the timing of switching to the second strike has a marked effect on the likelihood of driving the cancer to extinction, and that extinction therapy outperforms combination therapy when cross-resistance is present. We conduct an *in silico* trial that reveals when and why a second strike will succeed or fail. Finally, we demonstrate that our conclusions hold whether we model resistance as a binary trait or as a quantitative, multi-locus trait.

INTRODUCTION

Cancer is a heterogeneous collection of diseases with a wide variety of outcomes, natural histories and responses to therapy (Fidler 2012; Melo et al. 2013; Chen et al. 2014; Linnekamp et al. 2015; Shoag and Barbieri 2016; Kossaï et al. 2017). Cancerous neoplasms are often comprised of a diverse amalgamation of normal and malignant cells. A defining feature of cancerous cells is that they arise, divide, and proliferate uncontrollably as they adapt to their host environment through natural selection (Brown et al. 2023). Efforts to characterize the clonal evolutionary dynamics of cancer have been ongoing for decades (Farber 1990; Carreira et al. 2014; McFadden et al. 2014; Yu et al. 2014; Bhang et al. 2015; Jamal-Hanjani et al. 2017; Dang et al. 2020; Sandén et al. 2020; Huang et al. 2023). These efforts include experimental investigation of cancer's cellular kinetics (growth and death rates) and characterization of genetic changes during initial growth and following treatment. Cancer treatments such as immuno- and chemo-therapeutics pose a strong selective pressure on these populations of cells. Ideally, the effects of these drugs on cancer cell populations are strong enough to drive the cancer cells to extinction, but it is common for these populations to evolve resistance to treatment and then resume uncontrolled growth

(Wagle et al. 2011; Finn et al. 2012; Awad et al. 2021; Priest et al. 2023). Resistance to therapy represents a major obstacle to long-term progression free survival of patients. A better understanding of the evolutionary processes of cancer cell populations could lead to therapies that better mitigate or even exploit adaptive responses to treatment (Labrie et al. 2022). Modeling studies have proved useful for improving our understanding of the dynamics of cancer initiation, growth, and response to therapy (Cristini et al. 2003; Mallet and De Pillis 2006; Gatenby et al. 2007; Jeon et al. 2010; Sottoriva et al. 2010; Cook et al. 2016; Zangooei and Habibi 2017). Evolutionary models in particular help us understand when and why some treatment strategies will fail, and may inform new strategies (Mumenthaler et al. 2011; Beerenwinkel et al. 2015; Korobeinikov et al. 2017; Zhou et al. 2020; Pressley et al. 2021).

The interactions between a population and selective forces or environmental factors can be investigated using evolutionary and ecological models tailored for cancer, including those that describe the evolution of therapeutic resistance (reviewed in (Merlo et al. 2006) and (Laplane and Maley 2024)). For example, evolutionary rescue models (Gomulkiewicz and Holt 1995; Orr and Unckless 2008; Bell and Gonzalez 2009; Orr and Unckless 2014) define the patterns and dynamics of a population threatened with extinction due to a change in selection forces and the probability that that population will adapt sufficiently to avoid extinction and then subsequently recover. Evolutionary rescue occurs when a population is being driven towards extinction by unfavorable changes in the selective environment, but then a beneficial allele (or combination thereof) that is sufficient to mitigate or even benefit from this change becomes common in the population soon enough that the population can rebound before extinction. This results in a U-shaped trajectory of population size that is the hallmark of evolutionary rescue: initial rapid decline to a nadir, followed by renewed expansion (Orr and Unckless 2014).

Devising cancer treatment strategies with sustained effectiveness is in part tantamount to finding ways to prevent evolutionary rescue. In cancer, the population consists of the tumor cells, the selective force driving the population towards extinction is the therapy, and the beneficial allele is the mutation that confers drug resistance. Whether a tumor cell population in decline due to treatment will experience rescue depends on the chance that a resistant clonal subpopulation is established soon enough to prevent extinction. This in turn depends on the size of the cancer cell population at the onset of treatment, the rate at which the treatment kills cancer cells (which together determine how long it will take the cancer population to go extinct unless rescue occurs), and the mutation rate for resistance alleles. Higher mutation rates increase the probability that rescue will occur at any point in time. The presence of preexisting resistance mutations also increases the probability of evolutionary rescue (Orr and Unckless 2008). Thus, preventing evolutionary rescue demands therapeutic

regimes that maximize the selection against non-resistant tumor cells, while minimizing or delaying mutational events that give rise to resistance. For example, evolutionary rescue theory implies that combining multiple therapeutic drugs with independent modes of action can greatly improve patient outcomes because the rate of appearance of cells resistant to each drug in combination would typically be far lower than the mutation rate for resistance to a single drug. This notion is supported by the success of combination therapy in comparison to single therapy protocols (Labrie et al. 1993; Li et al. 2014; Mokhtari et al. 2017; Palmer and Sorger 2017; Fisusi and Akala 2019; Plana et al. 2022).

An alternative approach is “extinction therapy” (Gatenby et al. 2019; Gatenby et al. 2020; Gatenby and Brown 2020; Felder et al. 2021). Extinction therapy proposes that after a radical change in the environment resulting in a population crash, the population could be driven to extinction by a comparatively minor environmental perturbation that otherwise would not be a major threat. At the onset, extinction therapy resembles standard-of-care treatment: the most effective available therapy is initially used, continuing this treatment as long as it remains effective. Once the cancer cell population size has been dramatically reduced by the first-line treatment, a “second strike” is introduced with a different drug that may be less effective but is sufficient to push the now-threatened cancer cell population to extinction. Evolutionary modeling has shown that this “two-strike” extinction therapy can be effective (Gatenby et al. 2020; Patil et al. 2023), presuming the second strike is not too early (before the population has shrunk enough to be threatened by a less-effective treatment) or too late (once the population has been rescued by resistance to the first treatment and recovered to a large enough size to survive the second treatment).

Evolutionary modeling can answer outstanding fundamental questions about the conditions under which extinction therapy would be a superior approach, and how it should be carried out. Here we ask: how do factors like the mutation rate and the rate at which a therapy kills cancer cells influence the probability that a two-strike treatment will achieve extinction? What is the optimal timing of the second strike? Perhaps most importantly, when will simultaneous combination therapy be more effective than a sequential two-strike therapy, and vice versa?

Using population genetic simulations, we investigate the optimal timing of the second strike in an extinction therapy treatment protocol and compare the probability of extinction achieved by this sequential two-strike therapy with that of combination therapy. Our simulation approach reveals: 1) interactions between the optimal timing of two-strike sequential therapy, the mutation rate, and the rate at which the drug kills cancer cells; 2) the scenarios in which combination therapy outperforms optimally timed sequential extinction therapy and vice-versa, and 3) the implications of the genetic architecture of resistance (i.e., a binary trait caused by a single mutation vs. a

quantitative trait resulting from the cumulative effect of many mutations) for the optimal timing and effectiveness of a second strike.

METHODS

Several approaches have been used to model the growth, response to therapy, and clonal evolution of cancer. These include mathematical models (Dingli et al. 2006; Benzekry et al. 2014; Sun and Hu 2018; Zhang et al. 2022), spatial models (Thalhauser et al. 2010; Komarova 2013; Waclaw et al. 2015), and agent-based models (Wang et al. 2007; Zhang et al. 2009; Mustapha et al. 2016; Gong et al. 2017).

We used the software `SLiM 4.0` (Haller and Messer 2023) to simulate a diploid clonal population of cells undergoing expansion, treatment with two drugs, and mutations that confer resistance to these drugs. This software allows for agent-based evolutionary simulations which are widely used in the field of population genetics and provide a great deal of flexibility in modeling the evolution of resistance with minimal mathematical assumptions. Cells in these simulations have a specified genome size in base pairs and the simulation has a set mutation rate per base pair per cell cycle. To model clonal evolutionary dynamics, we set the recombination rate to 0. Events in the simulation occur over discrete generations (called cycles in SLiM), with the following events occurring sequentially during each generation (Figure S1):

1. Cell replication: Each cell initially undergoes mitotic replication, producing two daughter cells with the exact same genome (i.e. containing the same set of mutations) as the parent cell. Thus, the cancer cell population size doubles during this step.
2. Mutation: After cell division, each daughter cell may acquire new mutations that affect resistance to treatment (see step 3). Mutations can randomly occur at sites along the genome according to the mutation rate per base pair per cell cycle. If a mutation occurs, its type (e.g. conferring resistance to drug 1 vs. conferring resistance to drug 2) is determined according to a discrete probability distribution of mutation types, referred to as the draw rates. For instance, if the draw rates of two mutation types are (0.5, 0.5), then each mutation type is equally likely to be chosen.
3. Calculation of fitness costs: This step involves tallying the number of mutations in a cell and then calculating its fitness depending on the presence or absence of treatment during the current generation. Treatment reduces fitness, but resistance mutations can mitigate or eliminate this fitness cost. Cells may also die in the absence of treatment (“turnover”).
4. Death and survival: Next, the fitness costs incurred by each cell are used to calculate the probability of survival. At this step, each cell has a probability of

survival, P_{surv}, while the remaining cells die and thus removed from the simulation. Thus, the population contracts during this step, and cells that survive return to step one (replication) in the next cell cycle.

First model: two-strike extinction therapy in an evolutionary rescue model

A simulation begins with the expansion phase: a population starting with a single cell grows exponentially as described above until reaching a size of ~2^{20}. We note that this population size of about one million cells is smaller than the number of cells found in a clinically relevant tumor, but simulating smaller populations is a useful way of modeling the dynamics of larger populations while maintaining computational efficiency (but see (Dabi and Schrider 2024). Next comes the treatment phase, which consists of the application of the first drug for a specified number of time steps, followed by immediately switching to the second drug. The number of cell cycles during which the first drug is applied is referred to as the "second-strike lag time". Throughout the simulation, two types of mutations can occur: m1 and m2, which confer resistance to the first and second drugs, respectively. However, these mutations confer no fitness advantage or cost during the expansion and thus evolve under purely random drift throughout this phase. Note that we did not allow back-mutations: once a cell has acquired a given resistance mutation, all its descendants will harbor that same resistance allele.

In this model, resistance is a binary trait, and resistant cells do not experience any reduction in survival due to treatment nor due to any fitness tradeoff associated with resistance. The magnitude of the effect of each drug on the survival of non-resistant cells ("dose") during its treatment application is a tunable parameter. The equation governing survival probability during step 4 of each generation is as follows:

$$P_{surv} = (1 - r_{turnover}) \times \left(1 - dose_{drug_1} \times (1 - \mathbb{1}_{m1})\right) \times \left(1 - dose_{drug_2} \times (1 - \mathbb{1}_{m2})\right)$$

where:

$r_{turnover}$ is the turnover rate of cells. We set this to 0.20 for all simulations (i.e. 80% of cells survive in the absence of treatment)

$dose_{drug_1}$ is the dose of the first drug,

$dose_{drug_2}$ is the dose of the second drug,

$\mathbb{1}_{m1}$ is the indicator function that the cell has a mutation resistant to drug 1,

and $\mathbb{1}_{m2}$ is the indicator function that the cell has a mutation resistant to drug 2.

188 During the expansion phase, both drug doses are zero, meaning fitness is only
189 governed by the turnover rate. Application of either drug entails setting its dose to a
190 specified value > 0 while the other drug's dose remains at zero. The effect of each
191 drug's dose is to reduce the probability of survival, and the indicator resistance functions
192 govern whether a cell will experience this reduction in survival probability. Note that we
193 use the shorthand "drug" to refer to each treatment, but each of these treatments could
194 themselves be thought of as a combination of multiple drugs that together kills cancer
195 cells according to the specified dose parameter and to which resistance evolves at the
196 specified mutation rate.

197 We note that this simulation model differs from that of (Gatenby et al. 2020)
198 extinction therapy simulations in several key respects: 1) We model the two strikes in
199 the same manner in that they are continually applied drugs that each reduce the fitness
200 of cancer cells, while Gatenby et al. modeled the second strike as an instantaneous
201 40% reduction in the cancer cell population size rather than a continually applied
202 treatment; 2) We end treatment with the first drug at the moment the second strike
203 begins, whereas Gatenby et al.'s model continues therapy 1 after the second strike 3)
204 Gatenby et al. modeled resistance as a quantitative rather than binary trait (a change
205 we experiment with below); and 4) Gatenby et al.'s model includes an Allee effect, while
206 ours does not.

207 For our first set of simulations, we varied the mutation rate and second-strike lag
208 time to test the effect these parameters on treatment success. We tested per-base pair
209 mutation rates between 1.0×10^{-6} and 3.1×10^{-5} with increments of 2×10^{-6} and
210 second-strike lags between 1 and 20 cell cycles with increments of 1 cell cycle. Our
211 drug dose effects in these simulations were fixed at 0.75 for both drugs (i.e. 75% of
212 sensitive cells are killed by the drug each generation, on average). We ran 100
213 replicates of each parameter combination and measured the fraction of replicates in
214 which the population went extinct, which we refer to as the "fraction of extinct
215 replicates." We also tested the effect of using a lower dose of either drug across the
216 various mutation rates. Furthermore, we fixed the mutation rate and examined the effect
217 of varying both drug doses simultaneously.

218

219 **Fixed trajectories simulations**

220 In addition to examining sets of independent simulation replicates, we also conducted
221 an *in silico* trial examining how outcomes of two-strike extinction therapy differed among
222 a set of 55 *in silico* patients, where each patient is defined by a combination of mutation
223 rate and drug dose. Specifically, under a variant of our first model, we examined the
224 dynamics leading to extinction or evolutionary rescue for each patient by fixing the
225 trajectory of the population up to the time of applying the second treatment—this was

achieved by using a fixed initial random seed that was unique to that patient. Therefore, all replicates of patient share not only the drug dose and mutation rate, but the entire population trajectory up until the second treatment, including all birth and death events and mutations. When the second strike happens, a new replicate-specific random seed is chosen, producing stochastic trajectories after the second strike and allowing us to examine the distribution of treatment outcomes for each lag time for each synthetic patient.

Second model: the effect of combination therapy

We compared a combination therapy consisting of the simultaneous application of both drugs to sequential two-strike extinction therapy, again considering a range of second-strike lag times for the latter. In these simulations, combination therapy is simulated as both drugs having constant doses higher than zero throughout the treatment phase. The dose effects of both drugs in these simulations are always equal, and the lowest dose used for each drug in the combination was 0.4. We note that when both drug doses are 0.4, the survival probability of cells is still below 0.5 (see survival probability formula in Methods), meaning that a net decrease in population size is expected in the absence of resistance. For the two-strike simulations included in this comparison, we fix the dose effect of both drugs to 0.9, while varying this dose effect during combination therapy. We ran 100 replicates of each parameter combination.

Third model: cross-resistance

We modified the second model to include a third rare mutation type which confers resistance to both drugs. The draw rates for m1, m2, and m3 mutations under this third model are 45%, 45%, and 10% respectively. The survival probability under this model is:

$$P_{surv} = (1 - r_{turnover}) \times \left(1 - dose_{drug_1} \times (1 - \mathbb{1}_{m1})\right) \times \left(1 - \mathbb{1}_{m3} \times strength_{cross_resistance}\right) \times \left(1 - dose_{drug_2} \times (1 - \mathbb{1}_{m2})\right) \times \left(1 - \mathbb{1}_{m3} \times strength_{cross_resistance}\right)$$

This equation shows that the presence of cross-resistance mutations (i.e. $\mathbb{1}_{m3} = 1$) dampens the effect of both drugs on fitness in proportion to the strength of the cross-resistance. Here, a cell that lacks a mutation of type m1 or m2 can still be resistant to both drugs if it has a mutation of type m3, but rather than full resistance, the degree of resistance imparted by this mutation is determined by $strength_{cross_resistance}$; if $strength_{cross_resistance} = 0$ then m3 provides no resistance, but if

$strength_{cross_resistance} = 1$ then m3 confers full resistance to both drugs. We ran these simulations across a range of values of $strength_{cross_resistance}$, comparing the outcomes of combination therapy to sequential therapy with various lag times.

Fourth model: varying drug doses and the mutation rate ratio in combination therapy

To investigate whether the optimal combination of doses during combination therapy depends on the relative rates of mutation to resistance alleles for the two drugs, we carried out simulations with varying ratios of the rates of m1 and m2 mutations (achieved by varying the rate of m1 mutations while fixing the rate of m2 mutations). Specifically, we let the mutation rate for m1 mutations rage from 1×10^{-5} to $1.01 \times e^{-3}$ while the rate for m2 mutations was fixed to 1.5×10^{-5}. We also varied the ratio of the doses of the two drugs, under the constraint that $\left(1 - dose_{drug_1}\right) \times \left(1 - dose_{drug_2}\right)$ is fixed at 0.25. This was done by setting $dose_{drug_1}$ to a value between 0.30 and 0.70 and then setting $dose_{dru2}$ as follows:

$$dose_{drug_2} = 1 - 0.25/(1 - dose_{drug_1})$$

This ensures that the probability of survival for non-resistant cells is the same across all parameter combinations for this model. Any differences in extinction probability across parameterizations are therefore due to the interplay between drug mutation rates and drug doses.

Simulations modeling resistance as a quantitative trait

We also experimented with a model where drug resistance is a quantitative trait (Gomulkiewicz and Holt 1995). Cells can accumulate mutations conferring resistance to either drug. Each mutation contributes additively to resistance against the corresponding drug and its contribution is drawn from a lognormal distribution. The parameters of this distribution were chosen so that the average resistance effect of a new mutation was 0.1, meaning that, on average, 10 accumulated mutations of a specific type should confer full resistance to the corresponding drug. This yielded a mean of -2.42759 and a standard deviation of 0.5. The survival equation then becomes:

$$P_{surv} = (1 - r_{turnover}) \times \left(1 - dose_{drug_1} \times \left(1 - \sum_i W_{m1,i}\right)\right) \times \left(1 - dose_{drug_2} \times \left(1 - \sum_i W_{m2,i}\right)\right)$$

where:

294 $r_{turnover}$, $dose_{drug_1}$, and $dose_{drug_2}$ are as defined above,

295 $W_{m1,i}$ is the fitness effect of the m1 mutation at i (zero if no such mutation present),

296 and $W_{m2,i}$ is the fitness effect of the m1 mutation at i, if present. Thus, $\sum_i W_{m1,i}$ and
297 $\sum_i W_{m2,i}$ represent the cell's total amount of resistance to drugs 1 and 2, respectively

298 Note that under this model mutations can only increase resistance, and the
299 combined effect of all resistance mutations in a genome was capped at 1.

300

301 **RESULTS**

302 **Progression after treatment is a case of evolutionary rescue**

303 Typical cancer treatment involves applying the maximum tolerated dose (MTD) of a
304 first-line therapy until either the cancer is eradicated or until progression is observed
305 (Kareva et al. 2015). Progression often occurs because of the emergence of treatment-
306 resistant cells within the cancer cell population, which quickly propagate until the
307 remaining cells in the population are resistant to the treatment rendering it ineffective.
308 This is an example of evolutionary rescue, wherein a population is rapidly crashing
309 because of a change in the selective environment (i.e. treatment), but one or more
310 adaptive (e.g. resistance-conferring) mutations become common enough in the
311 population prior to extinction, thereby allowing the population to recover and eventually
312 progress beyond the size observed before treatment. A typical example of the trajectory
313 of a population undergoing evolutionary rescue is shown in Figure 1. In this example,
314 the population size is initially growing exponentially, but then rapidly declines following
315 the application of treatment. Eventually, the population size decreases to such a low
316 level that it may be undetectable. However, when the population is approaching its
317 nadir, a subpopulation of resistant cells emerges and begins to become more prevalent,
318 ensuring that the treatment will not succeed in eradicating the cancer.

319 Differences in treatment regime can alter the trajectory of evolutionary rescue.
320 Below we assess the efficacy of alternative treatment strategies that are designed to
321 reduce the probability of evolutionary rescue of the cancer cell population.

322

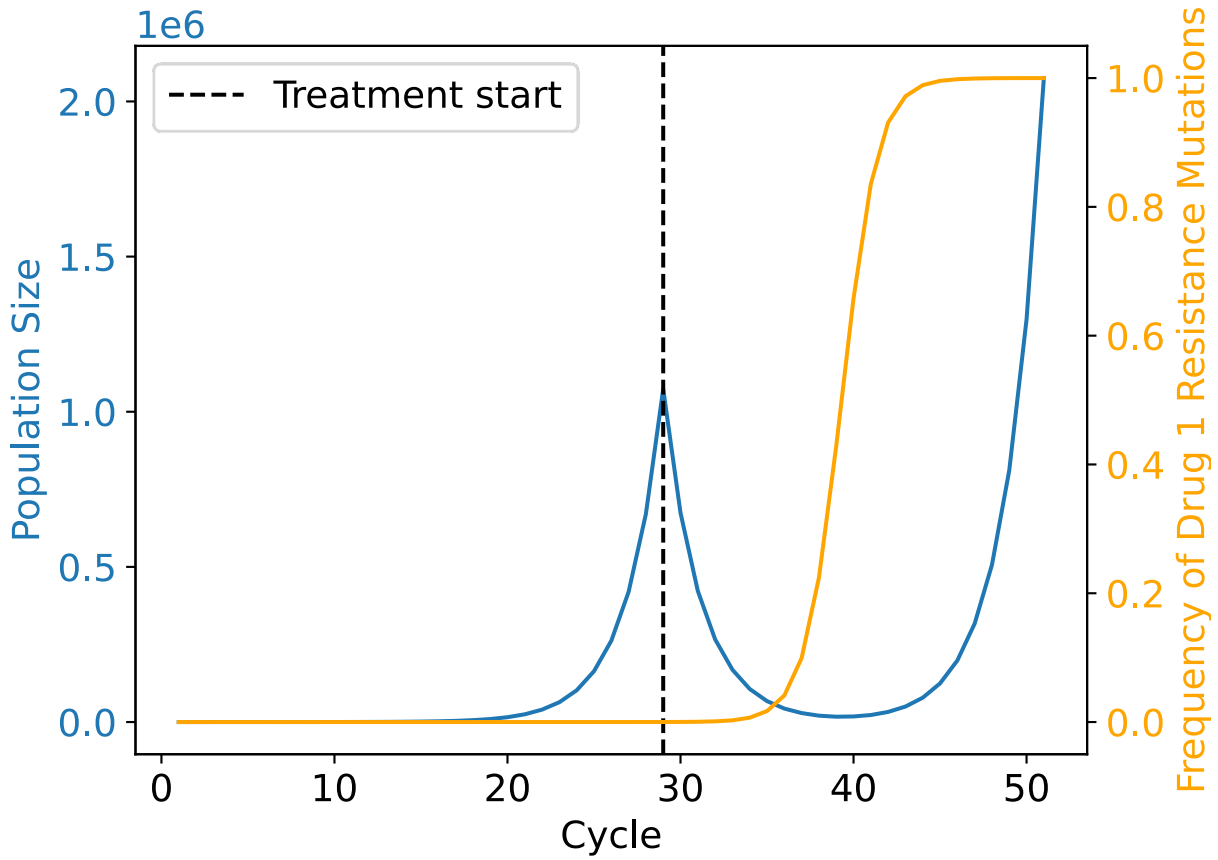

Figure 1. Trajectory of a cancer cell population during evolutionary rescue following treatment. The population expands exponentially (blue line) until the first strike therapy is applied (dashed black line), after which the population declines rapidly. However, as the population is declining, a resistance mutation has emerged and begun to increase in frequency in the population. As the treatment continues, the frequency of the resistance mutation continues to increase (orange line), the population eventually becomes fully resistant, resumes its exponential expansion, and ultimately recovers and progresses beyond its initial size pre-treatment. This is the classic U-shaped curve of evolutionary rescue. This example trajectory is taken from a single simulation replicate of our first model (Methods), but without the application of a second strike. For this replicate the mutation rate was set to 1.5×10^{-5} and the drug dose to ~0.61 (indicating that the fitness of treatment-sensitive cells is multiplied by ~0.39 during treatment; see Methods).

The optimal second-strike lag is independent of the mutation rate

In a two-strike cancer treatment scenario the timing of the change from the first-line to the second-line therapy may profoundly effect treatment success (Gatenby et al. 2020). We used simulations to estimate the probability of extinction across different timings of the second strike (the “second-strike lag time”) and different rates of mutation to treatment-resistance alleles to understand the relationship between second-strike lag

time and the probability that the cancer cell population will be driven to extinction. Our results (Figure 2A) show that there exists an optimal lag time between the onset of the first and second strikes for maximizing the extinction probability of the cell population. In general, the probability of extinction is low when the second drug is applied immediately following the application of the first (a lag time of only 1 cell cycle), then increases with greater lag times until an optimum is reached, and then decreases with increasing lag time. While there is no clear relationship between the mutation rate and the optimal lag time (Figure 2B), which remains generally between 7 and 9 cell cycles in our model, the mutation rate does exert an effect on the dynamics of population extinction probabilities across lag times. For instance, at lower mutation rates the extinction probability exhibits a broad plateau around the optimal lag time, implying that missing the optimal lag time is somewhat forgiving when resistance alleles do not frequently arise. As the mutation rate increases, however, the difference in extinction probability between the optimal lag time and suboptimal becomes starker, with a sharp peak around the optimum, and the extinction probability is also lower in general for all lag times.

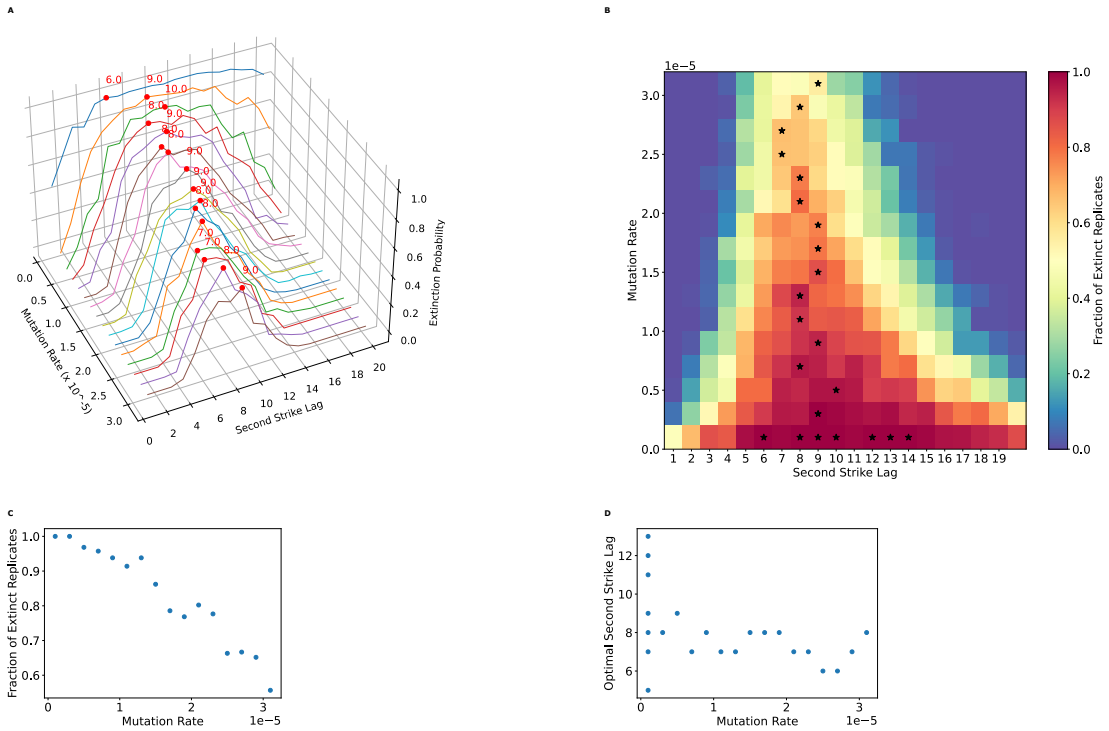

Figure 2. The optimal lag time is unaffected by resistance mutation rate, but the second strike is effective across a wider window of lag times when the mutation rate is lower. A) Extinction rate vs mutation rate and lag time. The *x*-axis represents the per base pair mutation rate of resistant mutations. The *y*-axis (Second Strike Lag) represents the time spent under the first treatment before switching to the second treatment. The *z*-axis (Extinction Probability) represents the fraction of replicates where the population went extinct. Red dots indicate the optimal lag time for each mutation rate (i.e. the lag time with the highest fraction of extinct replicates). The optimal lag time is relatively invariant across mutation rates. However, as the mutation rate increases, the difference in the extinction probability between the optimal lag time and other lag times becomes starker, and the extinction probability decreases for all lag times. B) The window for optimal strike is wider at lower mutations rates. Color indicates the extinction probability estimate and black stars at the optimal lag time(s) for each mutation rate—multiple stars are drawn in the case of a tie. C) The per-base pair mutation rate vs the extinction probability at the optimal lag time for that mutation rate. As the resistance mutation rate increases, the extinction probability decreases. D) Optimal second-strike lag vs mutation rate. This represents a 2D projection of the points indicated by the red dots in A. Despite some stochasticity present, the mutation rate is uncoupled from the optimal second-strike lag time. However, the window for the optimal time is wider for lower mutation rates (panel B), as multiple second-strike lag times produce a high extinction rate for the lower mutation rate.

More effective therapeutics should be used first during extinction therapy

The rate at which a population is being driven to extinction is a key determinant of the probability and timing of evolutionary rescue (Orr and Unckless 2008, 2014). We examined the effect of our drug dose parameters on extinction probabilities and optimal lag times by testing a scenario with a lower dose of drug 1 than drug 2, and one with a

lower dose of drug 2 than drug 1. In this context, drug doses control the reduction in fitness for non-resistant cells during the application of the drug (see Methods for fitness equation). When the first drug has a dose of 0.65 and the second a dose of 0.75, the optimal lag time shifts to around 10 generations (Figure 3A), versus 7–9 generations in the equal-dose effect scenario shown in Figure 2. This increase is likely due to the increased time required to shrink the population of cells enough for the second strike to result in extinction. Again, the mutation rate appears to have little effect on this optimal lag time, and extinction probabilities are lower for all mutation rates compared to the case where both drugs have a dose of 0.75.

Next, we examined the case where the first drug has a higher dose (0.75) than the second (0.65)—a scenario is more relevant to standard-of-care and to current thinking about extinction therapy (Gatenby et al. 2019) that advocates for using the drug with the highest kill rate as the first-line treatment. We found that optimal lag times in this scenario resemble those for the case in which both drugs had an equal dose of 0.75 and are also not dependent on mutation rate. However, the extinction probabilities across all mutation rates are higher compared to the case of the first drug having the lower dose (Figure 3B vs Figure 3A). For instance, at a mutation rate of 1.5×10^{-5}, simulations where both drugs have a dose of 0.75 result in an extinction probability of ~86% at an optimal lag time of 8, but this decreases to 0.53% when the first drug has a lower dose effect (in this case, at an optimal lag time of 11). On the other hand, reducing the dose effect of the second drug but not the first has hardly any effect on the outcome (extinction probability of ~85%, again with an optimal lag of 8). It is likely that the higher optimal lag time necessary to sufficiently reduce the population size when the first drug has a weaker effect also results in a higher likelihood of resistant mutants appearing. Thus, our results suggest using the stronger drug as the first strike during extinction therapy provides the best chance of eradicating the cancer cell population.

Finally, we set both drugs to an equal dose and examined extinction dynamics across various dose values (with the mutation rate set to 1.5×10^{-5} in each instance). When the dose of both drugs is equal, the optimal time increases as the drug dose decreases, and the extinction probability decreases from ~100% at a drug dose of 0.95 to ~20% at a drug dose of 0.60 (Figure 3C).

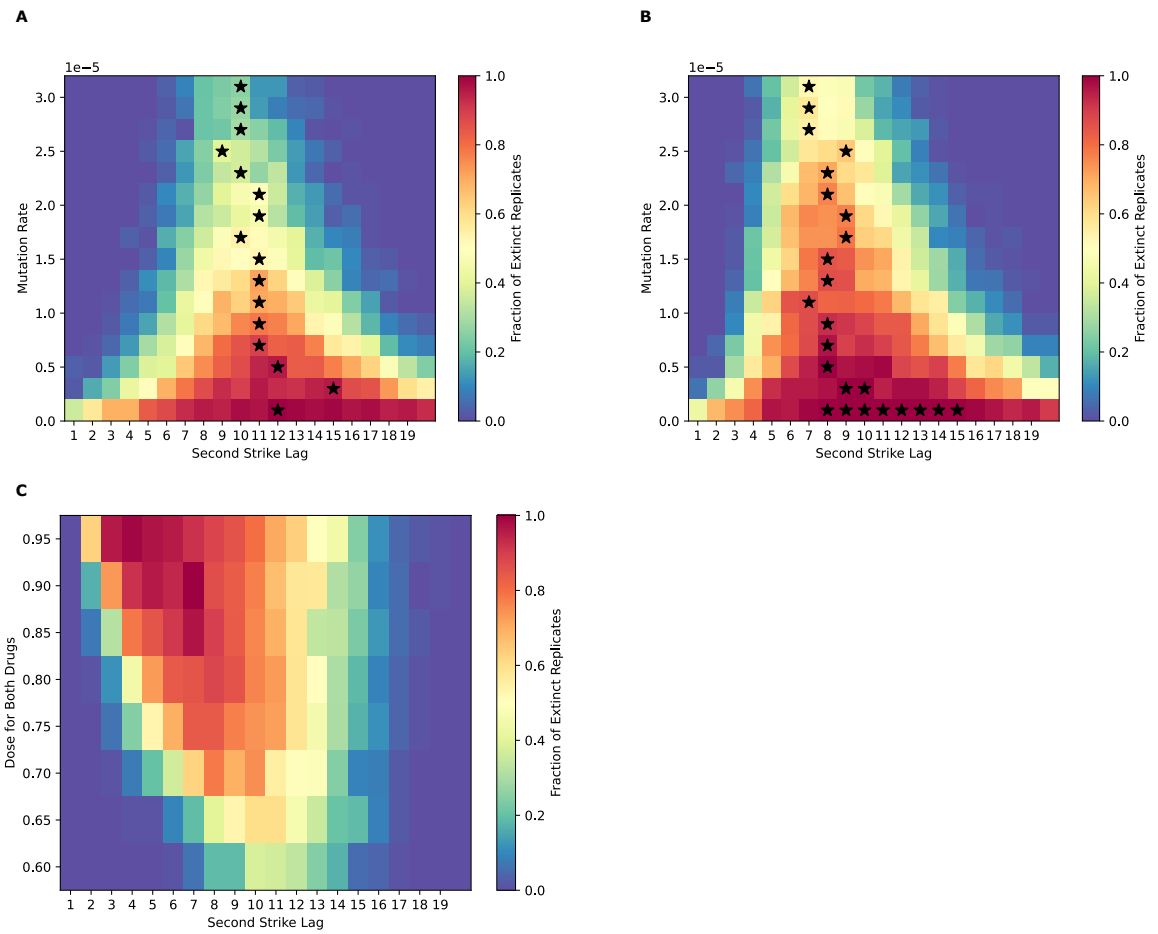

Figure 3. Using a lower-dose drug first reduces overall treatment success and shifts the optimal lag time higher. A) Extinction probability vs mutation rate and lag time when the first drug has a lower dose (0.65) before switching to a second drug with a higher dose (0.75). B) Extinction probability vs mutation rate and lag time when the first drug has a higher dose (0.75) followed by treatment with a second drug with a lower dose (0.65). D) Extinction probability vs lag time and the dose of both drugs when the mutation rate is fixed at 1.5×10^{-5}, with the dose always being equal for both drugs. Black stars represent the optimal lag time(s) at each mutation rate.

Investigating the dynamics of evolutionary rescue in extinction therapy via *in silico* trials

Extinction therapy succeeds when the first strike removes variants that confer resistance to the second strike

Our simulation approach allows us to go a step further and ask, for a given patient's disease course, what would have been the optimal treatment strategy? Such information would not only improve our understanding of the dynamics impacting the probability of extinction, but also help us assess the potential of treatment strategies

435 tailored to individual patients. To this end, we conducted an *in silico* trail with a set of
436 patients receiving two-strike extinction therapy, and determined, for each specific
437 patient, the optimal lag time. This may differ from patient to patient both because of
438 different parameter values (e.g. the mutation rate and drug dose parameters differ
439 across patients) and because of stochasticity in the timing of the emergence of
440 resistance and other random events occurring both before and during the treatment
441 course.

442 Our trial consisted of a set of 50 *in silico* patients, each of whom experienced a
443 deterministic disease trajectory up until the start of the second strike, at which point we
444 performed a set of 100 stochastic simulations to observe that patient's distribution of
445 outcomes for a given lag time (Methods). Illustrative example patients are shown in
446 Figure 4; the remainder are available on our project's GitHub repository. An examination
447 of these results reveals that two different, but related factors govern the probability of
448 treatment success (i.e. the fraction of extinct replicates) for a given lag time. The first is
449 the size of the cancer cell population at the time of the second strike, and second is the
450 frequency of the mutations at that time—results that are consistent with analytical
451 results (Orr and Unckless 2008). We therefore might expect the optimal lag time to be
452 the moment the population size is at its minimum (t_{min}), and indeed in many cases we
453 see that the extinction probability peaks when the second strike begins at t_{min}. Two such
454 examples are shown in Figure 4C and 4D; for these two synthetic patients a plateau of
455 extinction probability begins when the second strike starts at t_{min}.

456 However, beginning the second strike at t_{min} is not the optimal strategy for all
457 synthetic patients. This is because in some cases there is standing variation for
458 resistance to the second treatment present at t_{min}. Although they confer no fitness
459 benefit prior to the second strike, resistance mutations for the second drug typically
460 emerge during the expansion phase and persist at low frequency, and sometimes
461 remain present even as the population declines to its minimum size (see Figures 4A
462 and 4B for two such examples). In such cases, beginning the second strike at t_{min} will
463 almost always fail to achieve extinction. Instead, continuing the first treatment for one or
464 more cycles beyond t_{min} may reduce the frequency of these resistance mutations or
465 even remove them from the population, resulting in a much higher extinction probability.
466 This makes sense because, during the first strike, cells that are resistant to the first
467 treatment are selected for at the expense of others, including those that have
468 preexisting resistance to the second treatment, thereby reducing the chance of
469 evolutionary rescue following the second strike (e.g. Figures 4A, B).

470 <u>In silico *trials inform strategies for timing the second strike*</u>

471 Our synthetic trials also identify two-strike treatment strategies that are more likely to
472 prevent evolutionary rescue of the cancer cell population. For example, when examining

473 the results for all 50 synthetic patients, we find that switching to the second treatment at
474 the time where the population is at or near its minimum after the first strike is generally a
475 successful strategy (e.g. when the cancer cells' mutation rate is set to 6×10^{-6}, the
476 strategy of beginning the second strike at t_{min} results in an extinction probability that is
477 within 3% of its maximum for ~70% of synthetic patients).

478 In practice, however, it may not be possible to known t_{min}, until after the
479 population has begun to rebound. We therefore assessed the effectiveness of beginning
480 the second strike after some amount of time/growth after t_{min} is observed. First, we
481 assessed the effectiveness of beginning the second strike when the cell population has
482 grown either 10%, 50%, or 150% larger than its minimum size following application of
483 the first strike. This generally results in a high extinction probability (Figure 4E), but this
484 probability decreases from >90% to ~80% as we increase the amount of growth that we
485 allow to occur between t_{min} and the beginning of the second strike from 10% to 150%);
486 the variance in outcomes also increases with the amount of lag time post-t_{min}. Similarly,
487 applying the second strike after a specific number of cycles (i.e. 2, 3, or 4 cycles) after
488 t_{min} again yields generally good results (Figure 4F), although again efficacy decreases
489 and outcome variability increases as the amount of post-t_{min} lag time before the second
490 strike increases. In summary, our results suggest that while there may be variation in
491 outcomes from patient to patient, a second strike is most likely to be successful if it can
492 be initiated at or shortly after t_{min}.

493

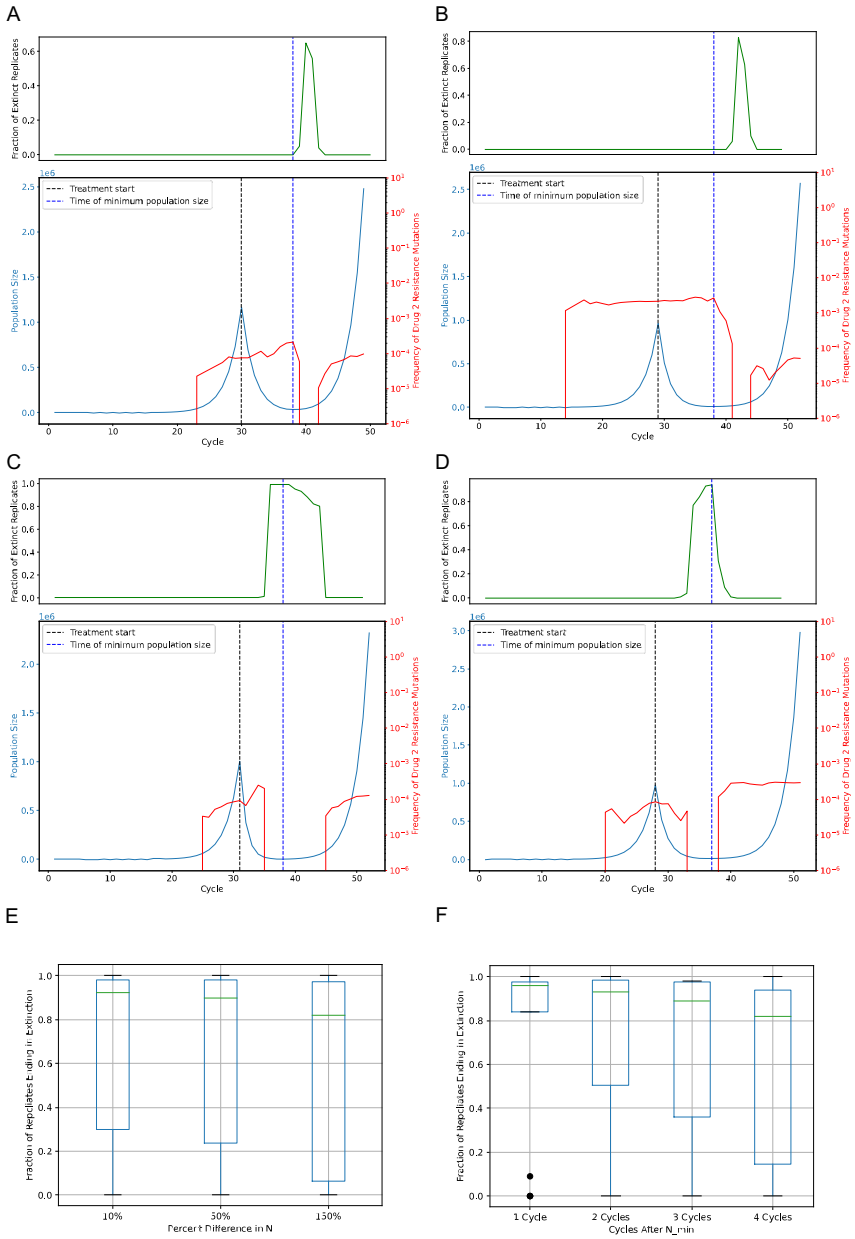

Figure 4. Synthetic patient trajectories show the success of strategies that involve switching treatments near the population nadir and the importance of eliminating standing variation. A-B) Trajectories of synthetic patients where the optimal lag time occurs after the time of minimum population size (dashed blue vertical line) due to remaining standing variation that confers resistance to the second treatment. C-D) Trajectories of synthetic patients where the optimal lag time is at the population minimum because standing variation that confers resistance to the second treatment has been eliminated prior to the population reaching its minimum. Blue lines represent the population size, red line represent the frequency of the mutation conferring resistance to the second strike, and green lines in the upper sub-panels represent the fraction of replicates that have undergone extinction when switching to the second strike at that time. Results for the remaining 46 in silico patients are available on our GitHub repository. E) The distribution of extinction probabilities for a separate set of validation patients across three different timing strategies for the second strike. Each value on the *x*-axis shows the percent growth in population

size over the size of the minimum population at the time of switching from the first strike to the second strike. F) The distribution of extinction probabilities for the set of validation patients across three more timing strategies for the second strike; each value on the *x*-axis shows the number of cycles allowed to occur after reaching the minimum population during the first strike before applying the second strike.

Combination therapy outperforms sequential therapy, except when cross-resistance is present

To compare the efficacy of combination therapy to optimally timed sequential therapy, we carried out simulations like those of the sequential therapy scenario above, but also included the possibility of combination therapy, wherein both drugs are applied simultaneously and at an equal dose until population rescue or extinction. We compared these simulations in the presence and absence of the possibility of mutations conferring cross-resistance to both drugs. Our results (Figure 5A) indicate that in the absence of cross-resistance combination therapy outperforms optimally timed sequential therapy for all combination drug doses above 0.4, with combination therapy failing to achieve extinction for any replicates when the dose of both drugs is 0.4. Furthermore, we note for all cases where the combination therapy dose is >0.40, the extinction probability does not increase substantially with increases in the combination drug dose, regardless of the mutation rate. Indeed, it is worth stressing that the combination therapy outperforms two-strike extinction therapy even though in most of these parameterizations the individual drugs used in the two-strike therapy kill cancer cells at a much higher rate than the combined effect of the drugs in the combination therapy. This implies that it is the much-reduced probability of independently evolving resistance to both drugs rather than an elevated rate of killing cancer cells that is responsible for the greater efficacy of the combination therapy approach under this model.

When cross-resistance mutations are present and the mutation rate is sufficiently high (Figure 5B), optimally timed sequential therapy outperforms combination therapy when the combination dose drugs are at 0.45, at all the tested strengths of cross-resistance. We also note that both therapies achieve extinction in only a small fraction of simulation replicates when the cross-resistance strength is high. This failure of treatment is more pronounced and occurs at even lower cross-resistance strengths when the mutation rate is 9×10^{-5} or higher. (See Figure S2 and Figure S3 for results at various mutation rates with and without cross-resistance). The lower probability of extinction under the sequential therapy at higher strengths of cross-resistance may be caused by cross-resistance mutations segregating at low frequency after the administration of the first drug. Such mutations are allowed to persist because the selective advantage of mutations conferring resistance to drug 1 over mutations conferring cross-resistance is diminished as the strength of cross resistance is

increased, resulting in preexisting resistance to the second drug at the time of the second strike.

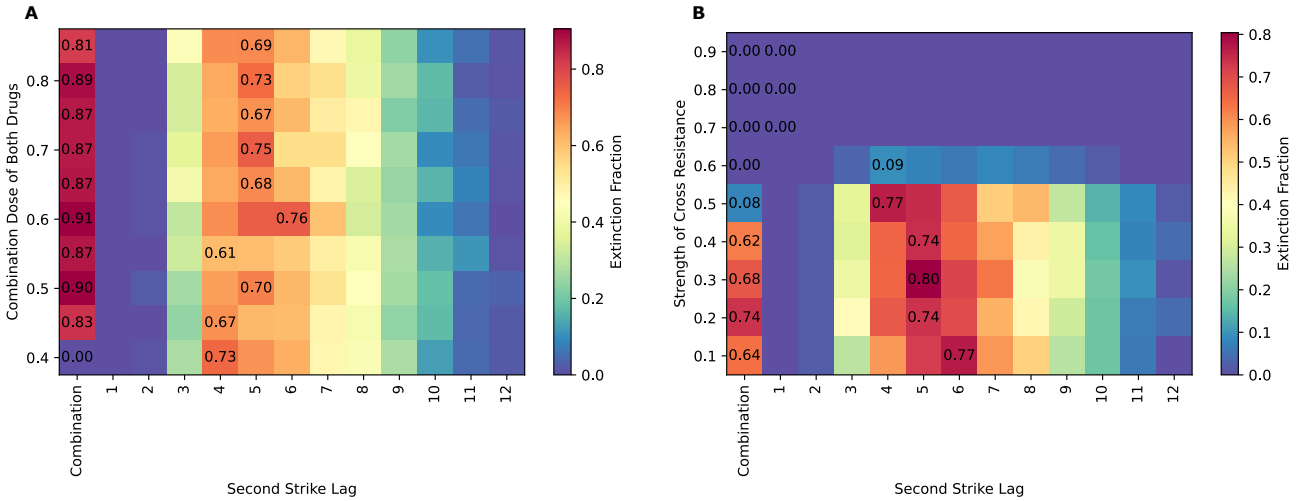

Figure 5. Comparison of efficacy between combination therapy and sequential therapy in the presence and absence of cross-resistance mutations shows that combination therapy is usually more effective except in cases of high cross resistance. A) Combination therapy and sequential therapy at a mutation rate of 5×10^{-5} in the absence of cross-resistance at various doses of combination drug. The sequential drug doses are fixed at 0.95 for both drugs. B) Combination therapy and sequential therapy at a mutation rate of 5×10^{-5} at various strengths of cross-resistance; the combination drug doses being fixed at 0.45 and the sequential drug doses are fixed at 0.95 for both drugs. The fraction of extinct replicates for the for the sequential protocol at the optimal time and for the combination protocol are indicated in black text. Combination therapy outperforms optimally timed sequential therapy at all doses of combination drugs, while sequential therapy outperforms combination therapy at the selected dose in the presence of cross mutations regardless of the strength of cross-resistance.

Equal drug doses in combination therapy are optimal regardless of resistance mutation rates

Given the importance of the mutation rate to combination therapy efficacy, we tested whether there is an optimal ratio of drug doses during combination therapy if the two resistant mutations have different mutation rates. To achieve this, we carried out simulations involving only combination therapy, fixing the mutation rate for resistance to the first drug and varying the mutation rate of resistance to the second drug. As outlined in the Methods, we varied the drug dose ratio but kept their combined effect constant so that the likelihood of death for treatment-sensitive cells was the same across all simulations. Our results (Figure S4) indicate that regardless of the difference in drug mutation rates, the highest chance of inducing population extinction is achieved when the doses of the two drugs in the combination is 1:1. This makes sense as this scenario

poses the greatest evolutionary challenge for the population in that both treatments need to be overcome to likely have significant rebound. Thus, our evolutionary rescue model suggests that it may be preferable to use a combination of treatments where each drug has a similar efficacy at killing cancer cells.

Extinction therapy dynamics appear largely similar if treatment resistance is a quantitative trait

So far, our simulations have treated resistance as a binary trait. Evolutionary rescue has also been modelled as a quantitative trait (Gomulkiewicz R, Holt RD. 1995) where resistance involves multiple loci of modest effect. We tested whether the results above hold in scenarios where resistance is conferred by the cumulative effect of multiple mutations. The contribution of each mutation to resistance was drawn from a lognormal distribution as described in the Methods. We find that an optimal lag time still exists in these simulations, and that it remains independent of the mutation rate for resistance (Figure S5A). However, the peaks of extinction probability around the optimal lag times are not as sharp as those in binary resistance simulations (compare to Figure 1).

We also examined the impact of varying drug doses under our under this quantitative trait model, and draw similar conclusions as under our binary trait model: optimal lag times are independent of mutation rates regardless of which drug has a lower dose, optimal lag times remain unchanged when drug 2 has the smaller dose, and optimal lag times are higher and extinction probabilities are lower when drug 1 has the smaller dose (Figure S5B, C, and D).

DISCUSSION

We performed forward-in-time agent-based population genetic simulations to evaluate the effectiveness of several different treatment strategies under an evolutionary rescue model. Under a sequential two-strike “extinction therapy” regime, we showed that the timing of the switch from the first drug to the second has a marked effect on the probability of the cell population going extinct (Figure 2). We also found that using the more effective drug first and the less effective drug second leads to substantially higher extinction probabilities than vice-versa (Figure 3). Furthermore, our simulations show that combination therapy forms a formidable barrier to the evolution of resistance when no mutations conferring cross-resistance exist, outperforming even optimally timed sequential therapy involving much stronger drugs than those used in the combination therapy (Figure 5A). This implies that combination therapies with lower doses may be preferable to sequential therapy using drugs that achieve a higher kill rate, because the probability of adapting to *each* drug in combination is very low so long as resistance

610 mechanisms are independent—this result is consistent with insights gained from studies
611 of pest control and antimicrobial treatment strategies (Pimentel and Burgess 1985;
612 Angst et al. 2021). We note that these results are in line with another potential benefit of
613 deploying combinations of drugs that attack different targets in a tumor cell: the time
614 and cost of developing and evaluating new treatments could be significantly reduced by
615 constructing a cocktail of existing pharmaceuticals rather than designing new drugs
616 (Mokhtari et al. 2017).

617 On the other hand, even drug combinations that target distinct pathways of a
618 cancer cell can often be overcome through a single mechanism that produces multidrug
619 resistance such as elevated xenobiotic metabolism, increased growth factor production,
620 etc. (Luqmani 2005; Bukowski et al. 2020). Our simulations show that when mutations
621 that confer sufficient levels of cross-resistance can occur, combination therapy can yield
622 worse outcomes than sequential therapy (Figure 5B). The superior effectiveness of two-
623 strike extinction therapy in this scenario is because, in situations where cross-resistant
624 mutations may be present but do not produce the same level of resistance as mutations
625 conferring resistance to a specific drug, the two-strike therapy will cause single-drug
626 resistance mutations to outcompete cross-resistant mutations, leaving the population
627 more vulnerable to the next drug in the sequence. However, as the degree of resistance
628 conferred by cross-resistance mutations approaches that of the single-drug resistance
629 mutations, the advantage of sequential therapy is erased and both approaches fail with
630 high probability. The failure of the two-strike approach here is most likely a result of the
631 persistence of segregating cross-resistant variants following the application of the first
632 drug which quickly render the second strike ineffective. We also show that with
633 combination therapies it is optimal to use drug dosing where each drug kills cancer cells
634 at the same rate, regardless of whether resistance to one drug arises at a higher rate
635 than the other. Overall, our results support the need for developing drug combinations
636 that are recalcitrant to the evolution of multidrug resistance (Pritchard et al. 2012), and
637 suggest that when cross-resistance cannot be avoided, two-strike extinction therapy
638 strategies may yield better outcomes.

639 We used *in silico* patient trials to investigate the evolutionary dynamics of two-
640 strike extinction therapy in greater detail. We found that for many patients the optimal
641 time to switch from the first to the second drug was at or near t_{min}, the time at which the
642 cancer cell population reaches its minimum and begins to rebound. Yet, the window of
643 opportunity to switch therapy following t_{min} may differ among patients. We do find that, if
644 one switches treatments shortly after t_{min}, the probability of extinction is often near its
645 maximum (Figure 4). However, we note that because the absolute amount of growth
646 occurring immediately after t_{min} is relatively minimal (Figure 1 and Figure 4), determining
647 t_{min} may not be feasible in practice until well after it has occurred. Thus, if one waits until
648 observable progression to initiate the second strike it may already be too late. We

649 therefore argue that efforts to accurately predict t_{min} for a given patient based on a
650 limited number of scans/assays may prove to be a better route toward improving patient
651 outcomes.

652 Our *in silico* trials show how adaptation to a treatment removes genetic diversity
653 that could confer resistance to a second treatment. It is for this reason that in those
654 patients for whom mutations conferring resistance to drug 2 were present at t_{min}, we
655 observed that the probability of extinction was very low if the second strike began at t_{min},
656 but much higher if the duration of the first strike was slightly extended in order to
657 remove these drug 2 resistance mutations. This illustrates that the success of two-strike
658 extinction therapy shares some similarity to the strategy of imposing an evolutionary
659 "double bind," wherein resistance to one treatment confers susceptibility to another
660 (Gatenby, Brown, et al. 2009; Basanta et al. 2012) although in our case this is a side
661 effect of the reduction in tumor heterogeneity caused by selection rather than a direct
662 phenotypic cost of resistance. In other words, the benefit of the first treatment is not only
663 to shrink the size of the cancer cell population, but also to reduce the amount of
664 diversity that could allow the population to immediately adapt to the second strike
665 (Messer and Petrov 2013). If treatments are switched too early, mutations conferring
666 resistance to the second strike may remain present in the cell population, while waiting
667 too long allows the population to rebound and allows mutations conferring resistance to
668 the second strike to randomly (re-)emerge in the population. Our results also imply that
669 the strategy of repeated changes to the selective environment (i.e. treating a patient
670 with a series of drugs used one after another in sequence) can further increase the
671 probability of extinction. This is consistent with previous theoretical studies that have
672 showed that frequent or continual environmental change can drive even initially very
673 robust and adaptable populations to extinction (Bürger and Lynch 1995; Orive et al.
674 2019). Indeed, if environmental stochasticity is present in addition to a major
675 environmental shift (i.e. treatment), extinction probability is further increased (e.g. (Xu et
676 al. 2023)), a fact that future treatment strategies may be able to exploit.

677 We note that our conclusions regarding the optimal timing of the second strike
678 are largely in agreement with those of a recent study by Patil et al. (2023) who
679 constructed an analytical model of evolutionary rescue under a similar two-strike
680 extinction therapy scenario as that examined here. Specifically, Patil et al. also found
681 that the nadir of the population after the first strike is usually the optimal point to switch
682 therapies, and that striking slightly after the nadir still yields good results. However, Patil
683 et al. found that including a cost of resistance induces a more complex relationship
684 where, if the second strike begins before the nadir, the extinction probability remains
685 high for a longer duration when the first drug's dose is intermediate and the second
686 drug's dose is high. This is because the population decline during the first strike is
687 slower if the drug dose is not too high, and this allows more time for selection against

cells resistant to the second drug, as these cells are experiencing the cost of resistance but no selective benefit. This result underscores the potential for resistance costs to qualitatively affect evolutionary dynamics during extinction therapy. The impact of the presence and strength of costs of resistance should thus be considered in future studies of not only the timing of two-strike extinction therapy but its relative efficacy vis-à-vis combination therapy.

Finally, the genetic architecture of resistance appears to have only modest implications for the effectiveness of sequential therapy. We observed similar dynamics whether treatment resistance is a binary trait or a quantitative trait where the degree of resistance is the sum of the effects of multiple mutations. However we note that in the latter scenario extinction probabilities display broader plateaus around the optimal lag times (Figure S5A). This may suggest that, all else being equal, sequential therapy involving treatments that exert highly polygenic selection on cancer populations may require less precision in the timing of the second strike, whereas treatments for which resistance is governed by a single locus may in some cases yield poor outcomes if the timing of the second strike misses the optimum by a relatively small period of time (Figure 2).

This study adds to the growing body of work showing that modeling the dynamics of evolutionary rescue can inform optimal treatment strategies and timings. The simulation approach that we adopted here is flexible. Our code can be easily adapted to model additional treatment strategies (e.g. adaptive therapy; (Gatenby, Silva, et al. 2009; Zhang et al. 2017; Zhang et al. 2022)) and to incorporate additional complexities into our model of cancer cell population evolution, adaptation, and extinction. Such features could include but are not limited to spatial heterogeneity and dynamics (Schmelz et al. 2021; Noble et al. 2022; Seferbekova et al. 2023), Allee effects (Boukal and Berec 2002; Konstorum et al. 2016; Brown et al. 2017; Gerlee et al. 2022), treatment refugia (Fu et al. 2015), non-genetic resistance mechanisms such as epigenetic responses (Bell and Gilan 2020) and transitions to drug-tolerant cell states (Sharma et al. 2010; Shaffer et al. 2017; Oren et al. 2021), and increasing rates of resistance mutations over time resulting from increased genomic instability (Lukow et al. 2021). Our agent-based simulation model could be readily extended to investigate these phenomena as well. More broadly, our study demonstrates the potential of flexible forward population genetic simulations of evolutionary rescue scenarios for investigating the dynamics of diverse treatment/management strategies for cancer and other diseases/organisms where the emergence of resistance is a common occurrence (e.g. antibiotic resistance, pesticide resistance, etc).

ACKNOWLEDGMENTS

The authors thank attendees of the Triangle Center for Evolutionary Medicine's 2023 Cancer and Evolution Catalysis Meeting for feedback on a preliminary version of this project.

FUNDING

DRS was supported by National Institutes of Health award R35GM138286, and AD was supported by the Royster Society of Fellows at the University of North Carolina at Chapel Hill. CDJ acknowledges the University Cancer Research Fund and the Lineberger Comprehensive Cancer Center Grant (P30CA016086) for support.

DATA AVAILABILITY

All code necessary for conducting the simulations carried out in this study can be found at https://github.com/SchriderLab/cancer_sims.

REFERENCES

Angst DC, Tepekule B, Sun L, Bogos B, Bonhoeffer S. 2021. Comparing treatment strategies to reduce antibiotic resistance in an in vitro epidemiological setting. Proceedings of the National Academy of Sciences. 118(13):e2023467118. doi:10.1073/pnas.2023467118.

Awad MM, Liu S, Rybkin II, Arbour KC, Dilly J, Zhu VW, Johnson ML, Heist RS, Patil T, Riely GJ, et al. 2021. Acquired Resistance to KRASG12C Inhibition in Cancer. N Engl J Med. 384(25):2382–2393. doi:10.1056/NEJMoa2105281.

Basanta D, Gatenby RA, Anderson ARA. 2012. Exploiting Evolution To Treat Drug Resistance: Combination Therapy and the Double Bind. Mol Pharmaceutics. 9(4):914–921. doi:10.1021/mp200458e.

Beerenwinkel N, Schwarz RF, Gerstung M, Markowetz F. 2015. Cancer Evolution: Mathematical Models and Computational Inference. Systematic Biology. 64(1):e1–e25. doi:10.1093/sysbio/syu081.

Bell CC, Gilan O. 2020. Principles and mechanisms of non-genetic resistance in cancer. Br J Cancer. 122(4):465–472. doi:10.1038/s41416-019-0648-6.

Bell G, Gonzalez A. 2009. Evolutionary rescue can prevent extinction following environmental change. Ecol Lett. 12(9):942–948. doi:10.1111/j.1461-0248.2009.01350.x.

Benzekry S, Lamont C, Beheshti A, Tracz A, Ebos JML, Hlatky L, Hahnfeldt P. 2014. Classical Mathematical Models for Description and Prediction of Experimental Tumor Growth. PLOS Computational Biology. 10(8):e1003800. doi:10.1371/journal.pcbi.1003800.

Bhang HC, Ruddy DA, Krishnamurthy Radhakrishna V, Caushi JX, Zhao R, Hims MM, Singh AP, Kao I, Rakiec D, Shaw P, et al. 2015. Studying clonal dynamics in response to cancer therapy using high-complexity barcoding. Nat Med. 21(5):440–448. doi:10.1038/nm.3841.

Boukal DS, Berec L. 2002. Single-species models of the Allee effect: extinction boundaries, sex ratios and mate encounters. J Theor Biol. 218(3):375–394. doi:10.1006/jtbi.2002.3084.

Brown JS, Amend SR, Austin RH, Gatenby RA, Hammarlund EU, Pienta KJ. 2023. Updating the Definition of Cancer. Mol Cancer Res. 21(11):1142–1147. doi:10.1158/1541-7786.MCR-23-0411.

Brown JS, Cunningham JJ, Gatenby RA. 2017. Aggregation Effects and Population-Based Dynamics as a Source of Therapy Resistance in Cancer. IEEE Trans Biomed Eng. 64(3):512–518. doi:10.1109/TBME.2016.2623564.

Bukowski K, Kciuk M, Kontek R. 2020. Mechanisms of Multidrug Resistance in Cancer Chemotherapy. International Journal of Molecular Sciences. 21(9):3233. doi:10.3390/ijms21093233.

Bürger R, Lynch M. 1995. EVOLUTION AND EXTINCTION IN A CHANGING ENVIRONMENT: A QUANTITATIVE-GENETIC ANALYSIS. Evolution. 49(1):151–163. doi:10.1111/j.1558-5646.1995.tb05967.x.

Carreira S, Romanel A, Goodall J, Grist E, Ferraldeschi R, Miranda S, Prandi D, Lorente D, Frenel J-S, Pezaro C, et al. 2014. Tumor clone dynamics in lethal prostate cancer. Science Translational Medicine. 6(254):254ra125-254ra125. doi:10.1126/scitranslmed.3009448.

Chen Z, Fillmore CM, Hammerman PS, Kim CF, Wong K-K. 2014. Non-small-cell lung cancers: a heterogeneous set of diseases. Nat Rev Cancer. 14(8):535–546. doi:10.1038/nrc3775.

Cook LM, Araujo A, Pow-Sang JM, Budzevich MM, Basanta D, Lynch CC. 2016. Predictive computational modeling to define effective treatment strategies for bone metastatic prostate cancer. Sci Rep. 6(1):29384. doi:10.1038/srep29384.

Cristini V, Lowengrub J, Nie Q. 2003. Nonlinear simulation of tumor growth. J Math Biol. 46(3):191–224. doi:10.1007/s00285-002-0174-6.

Dabi A, Schrider DR. 2024 Nov 6. Population size rescaling significantly biases outcomes of forward-in-time population genetic simulations. Genetics.:iyae180. doi:10.1093/genetics/iyae180.

Dang HX, Krasnick BA, White BS, Grossman JG, Strand MS, Zhang J, Cabanski CR, Miller CA, Fulton RS, Goedegebuure SP, et al. 2020. The clonal evolution of metastatic colorectal cancer. Science Advances. 6(24):eaay9691. doi:10.1126/sciadv.aay9691.

Dingli D, Cascino MD, Josić K, Russell SJ, Bajzer Ž. 2006. Mathematical modeling of cancer radiovirotherapy. Mathematical Biosciences. 199(1):55–78. doi:10.1016/j.mbs.2005.11.001.

Farber E. 1990. Clonal adaptation during carcinogenesis. Biochemical Pharmacology. 39(12):1837–1846. doi:10.1016/0006-2952(90)90599-G.

Felder SI, Fleming JB, Gatenby RA. 2021. Treatment-induced evolutionary dynamics in nonmetastatic locally advanced rectal adenocarcinoma. Adv Cancer Res. 151:39–67. doi:10.1016/bs.acr.2021.02.003.

Fidler IJ. 2012. Biological heterogeneity of cancer. Human Vaccines & Immunotherapeutics. 8(8):1141–1142. doi:10.4161/hv.19643.

Finn L, Markovic SN, Joseph RW. 2012. Therapy for metastatic melanoma: the past, present, and future. BMC Med. 10:23. doi:10.1186/1741-7015-10-23.

Fisusi FA, Akala EO. 2019. Drug Combinations in Breast Cancer Therapy. Pharmaceutical Nanotechnology. 7(1):3–23. doi:10.2174/2211738507666190122111224.

Fu F, Nowak MA, Bonhoeffer S. 2015. Spatial Heterogeneity in Drug Concentrations Can Facilitate the Emergence of Resistance to Cancer Therapy. PLoS Comput Biol. 11(3):e1004142. doi:10.1371/journal.pcbi.1004142.

Gatenby RA, Artzy-Randrup Y, Epstein T, Reed DR, Brown JS. 2020. Eradicating Metastatic Cancer and the Eco-Evolutionary Dynamics of Anthropocene Extinctions. Cancer Res. 80(3):613–623. doi:10.1158/0008-5472.CAN-19-1941.

Gatenby RA, Brown J, Vincent T. 2009. Lessons from Applied Ecology: Cancer Control Using an Evolutionary Double Bind. Cancer Research. 69(19):7499–7502. doi:10.1158/0008-5472.CAN-09-1354.

Gatenby RA, Brown JS. 2020. Integrating evolutionary dynamics into cancer therapy. Nat Rev Clin Oncol. 17(11):675–686. doi:10.1038/s41571-020-0411-1.

Gatenby RA, Silva AS, Gillies RJ, Frieden BR. 2009. Adaptive therapy. Cancer Res. 69(11):4894–4903. doi:10.1158/0008-5472.CAN-08-3658.

824 Gatenby RA, Smallbone K, Maini PK, Rose F, Averill J, Nagle RB, Worrall L, Gillies RJ. 2007.
825 Cellular adaptations to hypoxia and acidosis during somatic evolution of breast cancer. Br
826 J Cancer. 97(5):646–653. doi:10.1038/sj.bjc.6603922.

827 Gatenby RA, Zhang J, Brown JS. 2019. First Strike–Second Strike Strategies in Metastatic
828 Cancer: Lessons from the Evolutionary Dynamics of Extinction. Cancer Research.
829 79(13):3174–3177. doi:10.1158/0008-5472.CAN-19-0807.

830 Gerlee P, Altrock PM, Malik A, Krona C, Nelander S. 2022. Autocrine signaling can explain
831 the emergence of Allee effects in cancer cell populations. PLoS Comput Biol.
832 18(3):e1009844. doi:10.1371/journal.pcbi.1009844.

833 Gomulkiewicz R, Holt RD. 1995. WHEN DOES EVOLUTION BY NATURAL SELECTION
834 PREVENT EXTINCTION? Evolution. 49(1):201–207. doi:10.1111/j.1558-
835 5646.1995.tb05971.x.

836 Gong C, Milberg O, Wang B, Vicini P, Narwal R, Roskos L, Popel AS. 2017. A computational
837 multiscale agent-based model for simulating spatio-temporal tumour immune response to
838 PD1 and PDL1 inhibition. Journal of The Royal Society Interface. 14(134):20170320.
839 doi:10.1098/rsif.2017.0320.

840 Huang KK, Ma H, Chong RHH, Uchihara T, Lian BSX, Zhu F, Sheng T, Srivastava S, Tay ST,
841 Sundar R, et al. 2023. Spatiotemporal genomic profiling of intestinal metaplasia reveals
842 clonal dynamics of gastric cancer progression. Cancer Cell. 41(12):2019-2037.e8.
843 doi:10.1016/j.ccell.2023.10.004.

844 Jamal-Hanjani M, Wilson GA, McGranahan N, Birkbak NJ, Watkins TBK, Veeriah S, Shafi S,
845 Johnson DH, Mitter R, Rosenthal R, et al. 2017. Tracking the Evolution of Non–Small-Cell
846 Lung Cancer. New England Journal of Medicine. 376(22):2109–2121.
847 doi:10.1056/NEJMoa1616288.

848 Jeon J, Quaranta V, Cummings PT. 2010. An Off-Lattice Hybrid Discrete-Continuum Model
849 of Tumor Growth and Invasion. Biophysical Journal. 98(1):37–47.
850 doi:10.1016/j.bpj.2009.10.002.

851 Kareva I, Waxman DJ, Lakka Klement G. 2015. Metronomic chemotherapy: an attractive
852 alternative to maximum tolerated dose therapy that can activate anti-tumor immunity and
853 minimize therapeutic resistance. Cancer Lett. 358(2):100–106.
854 doi:10.1016/j.canlet.2014.12.039.

855 Komarova NL. 2013. Spatial stochastic models of cancer: Fitness, migration, invasion.
856 MBE. 10(3):761–775. doi:10.3934/mbe.2013.10.761.

857 Konstorum A, Hillen T, Lowengrub J. 2016. Feedback Regulation in a Cancer Stem Cell
858 Model can Cause an Allee Effect. Bull Math Biol. 78(4):754–785. doi:10.1007/s11538-016-
859 0161-5.

Korobeinikov A, Starkov KE, Valle PA. 2017. Modeling cancer evolution: evolutionary escape under immune system control. J Phys: Conf Ser. 811(1):012004. doi:10.1088/1742-6596/811/1/012004.

Kossaï M, Leary A, Scoazec J-Y, Genestie C. 2017. Ovarian Cancer: A Heterogeneous Disease. Pathobiology. 85(1–2):41–49. doi:10.1159/000479006.

Labrie F, Belanger A, Simard J, Labrie C, Dupont A. 1993. Combination therapy for prostate cancer. Endocrine and biologic basis of its choice as new standard first-line therapy. Cancer. 71(S3):1059–1067. doi:10.1002/1097-0142(19930201)71:3+<1059::AID-CNCR2820711426>3.0.CO;2-6.

Labrie M, Brugge JS, Mills GB, Zervantonakis IK. 2022. Therapeutic opportunities created by adaptive responses to targeted therapies in cancer. Nat Rev Cancer. 22(6):323–339. doi:10.1038/s41568-022-00454-5.

Laplane L, Maley CC. 2024. The evolutionary theory of cancer: challenges and potential solutions. Nat Rev Cancer. 24(10):718–733. doi:10.1038/s41568-024-00734-2.

Li F, Zhao C, Wang L. 2014. Molecular-targeted agents combination therapy for cancer: Developments and potentials. International Journal of Cancer. 134(6):1257–1269. doi:10.1002/ijc.28261.

Linnekamp JF, Wang X, Medema JP, Vermeulen L. 2015. Colorectal Cancer Heterogeneity and Targeted Therapy: A Case for Molecular Disease Subtypes. Cancer Research. 75(2):245–249. doi:10.1158/0008-5472.CAN-14-2240.

Lukow DA, Sausville EL, Suri P, Chunduri NK, Wieland A, Leu J, Smith JC, Girish V, Kumar AA, Kendall J, et al. 2021. Chromosomal instability accelerates the evolution of resistance to anti-cancer therapies. Developmental Cell. 56(17):2427-2439.e4. doi:10.1016/j.devcel.2021.07.009.

Luqmani YA. 2005. Mechanisms of drug resistance in cancer chemotherapy. Med Princ Pract. 14 Suppl 1:35–48. doi:10.1159/000086183.

Mallet DG, De Pillis LG. 2006. A cellular automata model of tumor–immune system interactions. Journal of Theoretical Biology. 239(3):334–350. doi:10.1016/j.jtbi.2005.08.002.

McFadden DG, Papagiannakopoulos T, Taylor-Weiner A, Stewart C, Carter SL, Cibulskis K, Bhutkar A, McKenna A, Dooley A, Vernon A, et al. 2014. Genetic and Clonal Dissection of Murine Small Cell Lung Carcinoma Progression by Genome Sequencing. Cell. 156(6):1298–1311. doi:10.1016/j.cell.2014.02.031.

Melo FDSE, Vermeulen L, Fessler E, Medema JP. 2013. Cancer heterogeneity—a multifaceted view. EMBO reports. 14(8):686–695. doi:10.1038/embor.2013.92.

Merlo LMF, Pepper JW, Reid BJ, Maley CC. 2006. Cancer as an evolutionary and ecological process. Nat Rev Cancer. 6(12):924–935. doi:10.1038/nrc2013.

Messer PW, Petrov DA. 2013. Population genomics of rapid adaptation by soft selective sweeps. Trends in Ecology & Evolution. 28(11):659–669. doi:10.1016/j.tree.2013.08.003.

Mokhtari RB, Homayouni TS, Baluch N, Morgatskaya E, Kumar S, Das B, Yeger H. 2017. Combination therapy in combating cancer. Oncotarget. 8(23):38022–38043. doi:10.18632/oncotarget.16723.

Mumenthaler SM, Foo J, Leder K, Choi NC, Agus DB, Pao W, Mallick P, Michor F. 2011. Evolutionary modeling of combination treatment strategies to overcome resistance to tyrosine kinase inhibitors in non-small cell lung cancer. Mol Pharm. 8(6):2069–2079. doi:10.1021/mp200270v.

Mustapha K, Gilli Q, Frayret J-M, Lahrichi N, Karimi E. 2016. Agent-based Simulation Patient Model for Colon and Colorectal Cancer Care Trajectory. Procedia Computer Science. 100:188–197. doi:10.1016/j.procs.2016.09.140.

Noble R, Burri D, Le Sueur C, Lemant J, Viossat Y, Kather JN, Beerenwinkel N. 2022. Spatial structure governs the mode of tumour evolution. Nat Ecol Evol. 6(2):207–217. doi:10.1038/s41559-021-01615-9.

Oren Y, Tsabar M, Cuoco MS, Amir-Zilberstein L, Cabanos HF, Hütter J-C, Hu B, Thakore PI, Tabaka M, Fulco CP, et al. 2021. Cycling cancer persister cells arise from lineages with distinct programs. Nature. 596(7873):576–582. doi:10.1038/s41586-021-03796-6.

Orive ME, Holt RD, Barfield M. 2019. Evolutionary Rescue in a Linearly Changing Environment: Limits on Predictability. Bull Math Biol. 81(11):4821–4839. doi:10.1007/s11538-018-0504-5.

Orr HA, Unckless RL. 2008. Population extinction and the genetics of adaptation. Am Nat. 172(2):160–169. doi:10.1086/589460.

Orr HA, Unckless RL. 2014. The Population Genetics of Evolutionary Rescue. PLOS Genetics. 10(8):e1004551. doi:10.1371/journal.pgen.1004551.

Palmer AC, Sorger PK. 2017. Combination Cancer Therapy Can Confer Benefit via Patient-to-Patient Variability without Drug Additivity or Synergy. Cell. 171(7):1678-1691.e13. doi:10.1016/j.cell.2017.11.009.

Patil S, Ahmed A, Viossat Y, Noble R. 2023. Preventing evolutionary rescue in cancer. doi:10.1101/2023.11.22.568336. [accessed 2025 Jan 8]. http://biorxiv.org/lookup/doi/10.1101/2023.11.22.568336.

Pimentel D, Burgess M. 1985. Effects of Single Versus Combinations of Insecticides on the Development of Resistance. Environmental Entomology. 14(5):582–589. doi:10.1093/ee/14.5.582.

Plana D, Palmer AC, Sorger PK. 2022. Independent Drug Action in Combination Therapy: Implications for Precision Oncology. Cancer Discovery. 12(3):606–624. doi:10.1158/2159-8290.CD-21-0212.

Pressley M, Salvioli M, Lewis DB, Richards CL, Brown JS, Staňková K. 2021. Evolutionary Dynamics of Treatment-Induced Resistance in Cancer Informs Understanding of Rapid Evolution in Natural Systems. Front Ecol Evol. 9. doi:10.3389/fevo.2021.681121. [accessed 2024 Nov 22]. https://www.frontiersin.org/journals/ecology-and-evolution/articles/10.3389/fevo.2021.681121/full.

Priest K, Le A, Gebregzabheir A, Nijmeh H, Reis GB, Mandell M, Davies KD, Lawrence C, O'Donnell E, Doebele RC, et al. 2023. Evolution of acquired resistance in a ROS1+ KRAS G12C+ NSCLC through the MAPK pathway. npj Precis Onc. 7(1):1–7. doi:10.1038/s41698-023-00349-0.

Pritchard JR, Lauffenburger DA, Hemann MT. 2012. Understanding resistance to combination chemotherapy. Drug Resistance Updates. 15(5):249–257. doi:10.1016/j.drup.2012.10.003.

Sandén C, Lilljebjörn H, Orsmark Pietras C, Henningsson R, Saba KH, Landberg N, Thorsson H, von Palffy S, Peña-Martinez P, Högberg C, et al. 2020. Clonal competition within complex evolutionary hierarchies shapes AML over time. Nat Commun. 11(1):579. doi:10.1038/s41467-019-14106-0.

Schmelz K, Toedling J, Huska M, Cwikla MC, Kruetzfeldt L-M, Proba J, Ambros PF, Ambros IM, Boral S, Lodrini M, et al. 2021. Spatial and temporal intratumour heterogeneity has potential consequences for single biopsy-based neuroblastoma treatment decisions. Nat Commun. 12(1):6804. doi:10.1038/s41467-021-26870-z.

Seferbekova Z, Lomakin A, Yates LR, Gerstung M. 2023. Spatial biology of cancer evolution. Nat Rev Genet. 24(5):295–313. doi:10.1038/s41576-022-00553-x.

Shaffer SM, Dunagin MC, Torborg SR, Torre EA, Emert B, Krepler C, Beqiri M, Sproesser K, Brafford PA, Xiao M, et al. 2017. Rare cell variability and drug-induced reprogramming as a mode of cancer drug resistance. Nature. 546(7658):431–435. doi:10.1038/nature22794.

Sharma SV, Lee DY, Li B, Quinlan MP, Takahashi F, Maheswaran S, McDermott U, Azizian N, Zou L, Fischbach MA, et al. 2010. A chromatin-mediated reversible drug-tolerant state in cancer cell subpopulations. Cell. 141(1):69–80. doi:10.1016/j.cell.2010.02.027.

Shoag J, Barbieri CE. 2016. Clinical variability and molecular heterogeneity in prostate cancer. Asian Journal of Andrology. 18(4):543. doi:10.4103/1008-682X.178852.

Sottoriva A, Verhoeff JJC, Borovski T, McWeeney SK, Naumov L, Medema JP, Sloot PMA, Vermeulen L. 2010. Cancer Stem Cell Tumor Model Reveals Invasive Morphology and Increased Phenotypical Heterogeneity. Cancer Research. 70(1):46–56. doi:10.1158/0008-5472.CAN-09-3663.

Sun X, Hu B. 2018. Mathematical modeling and computational prediction of cancer drug resistance. Briefings in Bioinformatics. 19(6):1382–1399. doi:10.1093/bib/bbx065.

Thalhauser CJ, Lowengrub JS, Stupack D, Komarova NL. 2010. Selection in spatial stochastic models of cancer: Migration as a key modulator of fitness. Biol Direct. 5(1):21. doi:10.1186/1745-6150-5-21.

Waclaw B, Bozic I, Pittman ME, Hruban RH, Vogelstein B, Nowak MA. 2015. A spatial model predicts that dispersal and cell turnover limit intratumour heterogeneity. Nature. 525(7568):261–264. doi:10.1038/nature14971.

Wagle N, Emery C, Berger MF, Davis MJ, Sawyer A, Pochanard P, Kehoe SM, Johannessen CM, MacConaill LE, Hahn WC, et al. 2011. Dissecting Therapeutic Resistance to RAF Inhibition in Melanoma by Tumor Genomic Profiling. J Clin Oncol. 29(22):3085–3096. doi:10.1200/JCO.2010.33.2312.

Wang Z, Zhang L, Sagotsky J, Deisboeck TS. 2007. Simulating non-small cell lung cancer with a multiscale agent-based model. Theor Biol Med Model. 4(1):50. doi:10.1186/1742-4682-4-50.

Xu K, Vision TJ, Servedio MR. 2023. Evolutionary rescue under demographic and environmental stochasticity. J Evol Biol. 36(10):1525–1538. doi:10.1111/jeb.14224.

Yu H, Han Z, Wang Y, Xin H. 2014. The Clonal Evolution and Therapeutic Approaches of Lung Cancer. Cell Biochem Biophys. 70(1):63–71. doi:10.1007/s12013-014-9910-y.

Zangooei MH, Habibi J. 2017. Hybrid multiscale modeling and prediction of cancer cell behavior. PLOS ONE. 12(8):e0183810. doi:10.1371/journal.pone.0183810.

Zhang J, Cunningham J, Brown J, Gatenby R. 2022. Evolution-based mathematical models significantly prolong response to abiraterone in metastatic castrate-resistant prostate cancer and identify strategies to further improve outcomes. Perry GH, editor. eLife. 11:e76284. doi:10.7554/eLife.76284.

Zhang J, Cunningham JJ, Brown JS, Gatenby RA. 2017. Integrating evolutionary dynamics into treatment of metastatic castrate-resistant prostate cancer. Nat Commun. 8(1):1816. doi:10.1038/s41467-017-01968-5.

Zhang L, Wang Z, Sagotsky JA, Deisboeck TS. 2009. Multiscale agent-based cancer modeling. J Math Biol. 58(4):545–559. doi:10.1007/s00285-008-0211-1.

Zhou J, Liu Y, Zhang Y, Li Q, Cao Y. 2020. Modeling Tumor Evolutionary Dynamics to Predict Clinical Outcomes for Patients with Metastatic Colorectal Cancer: A Retrospective Analysis. Cancer Res. 80(3):591–601. doi:10.1158/0008-5472.CAN-19-1940.